The Astrophysical Journal, 640: L1–L4, 2006 March 20

INTERFEROMETRIC 890 μm IMAGES OF HIGH-REDSHIFT SUBMILLIMETER GALAXIES

D. Iono,[1,2] A. B. Peck,[1] A. Pope,[3] C. Borys,[4] D. Scott,[3] D. J. Wilner,[1] M. Gurwell,[1] P. T. P. Ho,[1] M. S. Yun,[5] S. Matsushita,[6] G. R. Petitpas,[1] J. S. Dunlop,[7] M. Elvis,[1] A. Blain,[4] and E. Le Floc'h[8]

Received 2005 August 19; accepted 2006 February 9; published 2006 March 1

ABSTRACT

We present high-resolution 890 μm images of two 20 mJy submillimeter galaxies, SMM J123711+622212 and MIPS J142824.0+352619, obtained using the Submillimeter Array (SMA). Using submillimeter interferometric observations with an angular resolution of 2.″5, the coordinates of these high-redshift sources are determined with an accuracy of 0.″2. The new SMA data on SMM J123711+622212 reveal an unresolved submillimeter source offset to the east by 0.″8 from an optical galaxy found in deep *HST* images, suggesting either a large galaxy with a dusty central region or an interacting galaxy system. The SMA image of hyperluminous ($L_{\rm FIR} = 3.2 \times 10^{13}\,L_{\odot}$) source MIPS J142824.0+352619 provides a firm upper limit to the source size of $\lesssim$1.″2. This constraint provides evidence that the foreground lens is only weakly affecting the observed high far-infrared luminosity.

Subject headings: cosmology: observations — galaxies: formation — galaxies: high-redshift — galaxies: starburst — submillimeter

1. INTRODUCTION

The discovery of high-redshift submillimeter sources has significantly improved our understanding of the star formation history in the early universe. Negative *k*-correction allows one to observe the thermal dust emission at 850 μm almost independent of the redshift up to $z \sim 10$ (Blain et al. 2002). Deep observations using the SCUBA bolometer on the James Clerk Maxwell Telescope (JCMT) have unveiled the presence of distant submillimeter sources (Smail et al. 1997; Barger et al. 1998; Hughes et al. 1998; Eales et al. 2000; Cowie et al. 2002; Scott et al. 2002; Borys et al. 2003; Webb et al. 2003; Wang et al. 2004). The primary origin of the submillimeter emission is believed to be the reprocessed dust emission from newborn stars in young galaxies. While these discoveries are attended by a great number of high-resolution follow-up optical/NIR imaging studies, the 14″ resolution of the JCMT at 850 μm yields a large error circle that is too coarse for a precise determination of the optical/NIR counterparts to these sources. Deep optical imaging typically shows several optical/NIR sources within the SCUBA beam. To date, the most successful ways to obtain precise astrometry on the target are to obtain high-resolution, deep 1.4 GHz radio images (Ivison et al. 1998; Barger et al. 2000; Chapman et al. 2001; Ivison et al. 2002; Dunlop et al. 2004) or to obtain interferometric 1.3 mm continuum images (e.g., Downes et al. 1999). The former, however, does not identify robust optical/NIR counterparts for all of the sources, revealing counterparts for ~75% of the $S_{850\,\mu{\rm m}} > 5$ mJy sources with $S_{1.4\,{\rm GHz}} > 30$ μJy (e.g., Ivison et al. 2002; Chapman et al. 2003; Borys et al. 2004; Greve et al. 2004; Wang et al. 2004). Precise astrometry obtained using millimeter or submillimeter interferometers allows us to unambiguously identify the correct counterpart for the remaining radio-faint sources and for sources with multiple radio counterparts. High angular resolution submillimeter observations also allow us to understand the true nature of the submillimeter sources with established optical counterparts in which gravitational lensing is a possibility.

We present recent Submillimeter Array (SMA; Ho et al. 2004) detections of two $S_{850\,\mu{\rm m}} \sim 20$ mJy sources, SMM J123711+622212 (hereafter GN 20; Pope et al. 2005) and MIPS J142824.0+352619 (hereafter MIPS-J1428; Borys et al. 2006). The 20.3 mJy source GN 20 was discovered in the recent SCUBA observations of the GOODS-North field (Giavalisco et al. 2004). GN 20, with its 10 σ 850 μm detection (Pope et al. 2005) and 5 σ 1.3 mm detection at the IRAM Plateau de Bure Interferometer (PdBI; A. Pope et al. 2006, in preparation), is one of the strongest submillimeter sources discovered to date. It has very weak radio and undetectable 450 μm emission, suggesting it lies at high redshift.

MIPS-J1428 was discovered in the Multiband Imaging Photometer for *Spitzer* (MIPS) images of the NOAO Deep Wide Field Survey (NDWFS) Bootes field (Jannuzi & Dey 1999; Soifer et al. 2004). It was detected (Borys et al. 2006) at 350 μm using SHARC II (Dowell et al. 2003) on the Caltech Submillimeter Observatory, 1.4 GHz radio continuum at the Very Large Array (VLA), and subsequent follow-up observations (Borys et al. 2006) revealed that it is an extremely luminous [$(3.2 \pm 0.7) \times 10^{13}\,L_{\odot}$] starburst-dominated galaxy at $z = 1.325$. Recent Keck-DEIMOS spectroscopy has revealed a $z = 1.034$ galaxy directly aligned with MIPS-J1428 (Borys et al. 2006), possibly lensing it. High angular resolution submillimeter observations allow us to determine whether or not the submillimeter emission is coincident with the optical emission, and thereby search for any evidence for amplification of the far-infrared (FIR) luminosity by gravitational lensing. We adopt $H_0 = 70$ km s^{-1} Mpc^{-1}, $\Omega_m = 0.3$, and $\Omega_\Lambda = 0.7$.

[1] Harvard-Smithsonian Center for Astrophysics, 60 Garden Street, Cambridge, MA 02138.
[2] National Astronomical Observatory of Japan, 2-21-1 Osawa, Mitaka, 181-8588 Tokyo, Japan; d.iono@nao.ac.jp.
[3] Department of Physics and Astronomy, University of British Columbia, Vancouver, BC V6T 1Z1, Canada.
[4] California Institute of Technology, Pasadena, CA 91125.
[5] Department of Astronomy, University of Massachusetts, Amherst, MA 01003.
[6] Academia Sinica Institute of Astronomy and Astrophysics, P.O. Box 23-141, Taipei 106, Taiwan.
[7] Institute for Astronomy, University of Edinburgh, Royal Observatory, Blackford Hill, Edinburgh EH9 3HJ, UK.
[8] Steward Observatory, 933 North Cherry Avenue, Tucson, AZ 85721.

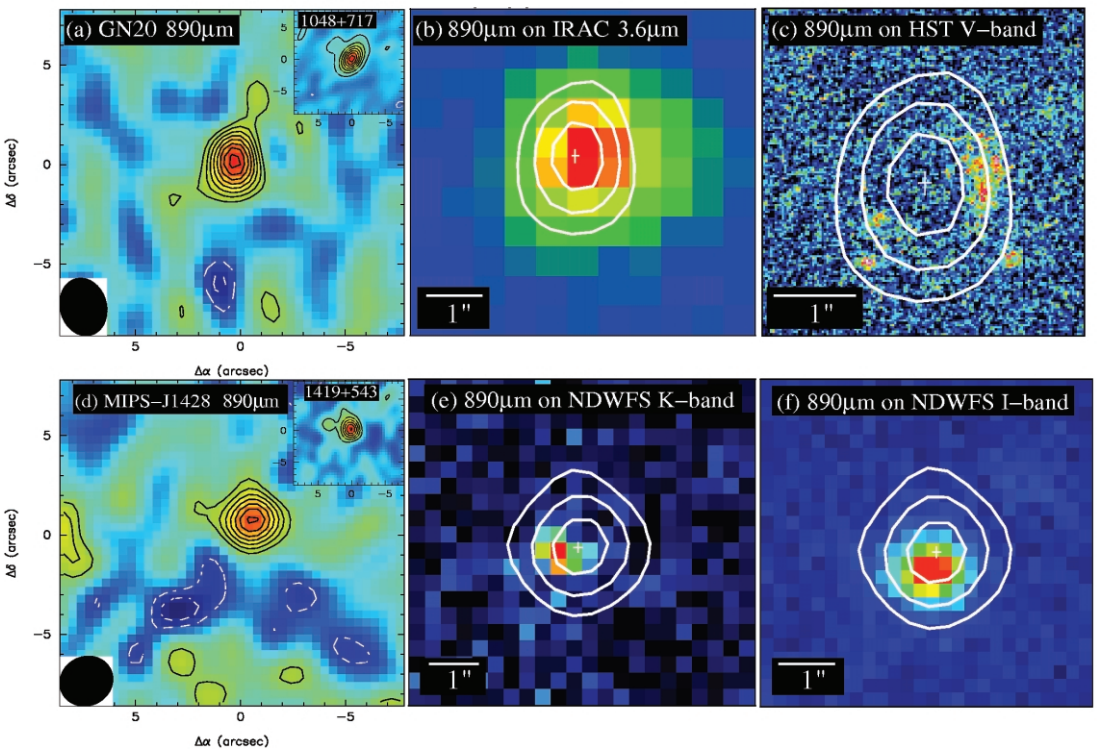

FIG. 1.—(*a*) SMA 890 μm map of GN 20 and 1048+717 (*inset*). The lowest positive contours represent 2 σ, and the contours increase by 1 σ for GN 20 and by 2 σ for 1048+717. The lowest negative contour is 2 σ and increases by 1 σ. (*b*) SMA 890 μm contours overlaid on the *Spitzer* IRAC 3.6 μm image and over the (*c*) *HST* ACS *V*-band image, both obtained from the GOODS archive. The IRAC and *HST* images are corrected for the known 0.″38 offset in declination. The 4, 6, and 8 σ contours from (*a*) are shown, and error bars near the center show the astrometric accuracy of the SMA image. (*d*) SMA map of MIPS-J1428 and 1419+543 (*inset*). The contours are the same as in GN 20. The smallness of the astrometric errors (0.″1–0.″2) from the phase center in the 1048+717 and 1419+543 maps proves the robustness of the astrometry of GN 20 and MIPS-J1428. The SMA 890 μm map of MIPS-J1428 is shown overlaid on the NDWFS (*e*) *K*-band image and the (*f*) *I*-band image. The 3, 5, and 7 σ contours from (*d*) are shown, and error bars near the center show the astrometric accuracy of the SMA image.

2. OBSERVATION AND DATA REDUCTION

GN 20 was observed on 2005 February 20 (track 1) and March 5 (track 2), and MIPS-J1428 was observed on 2005 March 8 (track 3) and April 4 (track 4) using 5–7 antennas in the compact configuration of the SMA. The SIS receivers were tuned to a center frequency of 342.883 GHz in the upper sideband (USB), yielding 332.639 GHz in the lower sideband (LSB). This tuning frequency was chosen to facilitate the receiver tuning and to achieve the optimal receiver performance. The target coordinates were obtained from the 1.3 mm IRAM PdBI detection of GN 20 [α(J2000) = $12^h37^m11\overset{s}{.}88$, δ(J2000) = 62°22′12.″00; A. Pope et al. 2006, in preparation] and the position of the proposed MIR galaxy of MIPS-J1428 [α(J2000) = $14^h28^m24\overset{s}{.}10$, δ(J2000) = 35°26′19.″00; Borys et al. 2006]. All tracks were taken under good atmospheric opacity (i.e., τ_{225} = 0.04–0.08).

The SMA data were calibrated using the Caltech software package MIR, modified for the SMA. Antenna-based pass-band calibration was done using all of the planets and bright QSOs observed in a given track. For GN 20, antenna-based time-dependent phase calibration was done using 1153+495, a 0.7 Jy QSO 14° away from the target. In addition, a 0.6 Jy QSO near GN 20, 1048+717 (14° from GN 20, 23° from 1153+495) was observed for a total of 12 minutes during each track. The detection of 1048+717 at the phase center empirically verifies and constrains the accuracy of the phase calibration referenced to 1153+495 (see § 3). Similarly for the MIPS-J1428 tracks, two QSOs, 1310+323 (0.6 Jy; 16° away from MIPS-J1428) and 1635+381 (1.0 Jy; 25° away from MIPS-J1428), were used together to calibrate the time-dependent phase, and 1419+543 (0.4 Jy; 3° away from MIPS-J1428) was used to check the astrometry. Finally, absolute flux calibration was performed using Callisto and Mars. Imaging was carried out in MIRIAD (Sault et al. 1995). Maximum sensitivity was achieved by adopting natural weighting, which gave a synthesized beam size of 2.″9 × 2.″2 (P.A. = 12.°2) for GN 20 and 2.″6 × 2.″4 (P.A. = −47.°2) for MIPS-J1428. The rms noise after combining the two sidebands in two tracks was 2.1 mJy (GN 20) and 2.2 mJy (MIPS-J1428).

3. RESULTS AND DISCUSSION

3.1. *SMM J123711+622212 (GN 20)*

The SMA image of GN 20 is shown in Figure 1*a*. The real part of the visibility amplitudes does not decline as a function of projected baseline length, indicating that the emission is not spatially resolved (Fig. 2). The upper limit on the source size is 1.″2. The derived total flux from a point-source model is 22.9 ± 2.8 mJy, consistent with the 890 μm flux of 18.1 mJy extrapolated from the SCUBA 850 μm flux of 20.3 ± 2.1 mJy (Pope et al. 2005). The derived coordinates for GN 20 are α(J2000) = $12^h37^m11\overset{s}{.}92$, δ(J2000) = 62°22′12.″10, with statistical uncertainties in the fit of 0.″1 for both α and δ. These are consistent with estimated errors of ∼0.″11 in α and ∼0.″15 in δ from a 10 σ detection and a beam of 2.″9 × 2.″2.

In order to check the robustness of our phase calibration and to estimate the systematic uncertainties in the SMA astrometry,

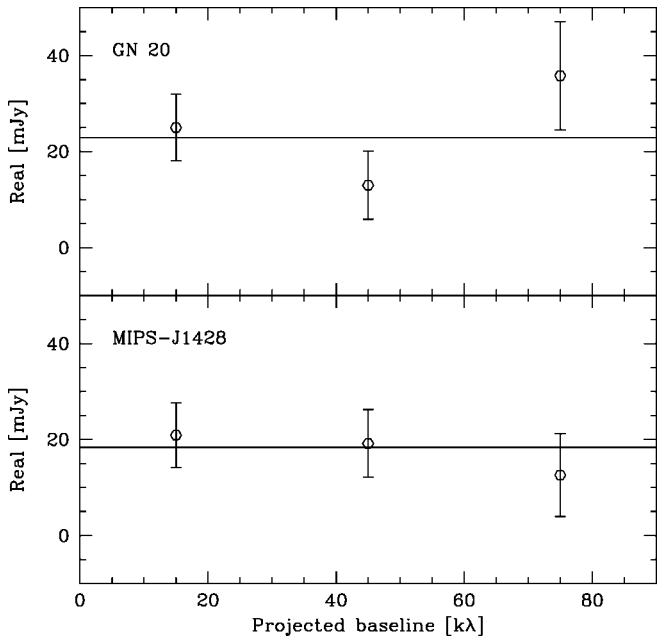

FIG. 2.—Real part of the visibility amplitudes vs. projected baseline length for GN 20 (*top*) and MIPS-J1428 (*bottom*). The solid horizontal lines represent a point-source model with continuum fluxes of 22.9 mJy (GN 20) and 18.4 mJy (MIPS-J1428). The upper limit to the source sizes of both of these sources are comparable to the scale constrained by the longest baseline length, which is ~1″.2.

we have imaged the test QSO (1048+717) using the same phase calibration we used to map GN 20. The resultant QSO map after adding the two sidebands and two tracks is shown in the inset of Figure 1*a*. A point-source fit to the visibilities of 1048+717 gave a positional offset from the phase center of $\Delta\alpha = 0''.01 \pm 0''.02$ and $\Delta\delta = 0''.06 \pm 0''.02$. The coordinates of this and all of the QSOs used in these observations were adopted from the radio reference frame (Johnston et al. 1995), and they are accurate to better than 3 mas. Hence, the precise detection of 1048+717 at the phase center ensures that our phase calibration referenced to 1154+379 is robust.

As an additional check, we fit a point-source model to the visibilities of 1048+717 in each sideband of each track separately. The results show that the offsets from the phase center are consistent among the different sidebands and tracks in right ascension ($\Delta\alpha = 0''.01$–$0''.04$), slightly larger in declination for track 2 ($\Delta\delta = 0''.02$–$0''.05$), and a factor 10 larger in declination for track 1 ($\Delta\delta \sim 0''.30$). The overall average offset from the phase center is $\Delta\alpha = 0''.02 \pm 0.02$ and $\Delta\delta = 0''.16 \pm 0.14$. The uncertainties in declination in track 2 are larger than the uncertainties in right ascension due to beam elongation in the north-south direction, while the source of the factor 10 larger error in track 1 is not obvious from the data. These errors are consistent with the uncertainties of 0″.1–0″.15 expected from a maximum baseline error of 0.1 λ at 230 GHz using a phase calibrator that is 15° away from the target. These systematic tests prove the robustness of our phase calibration in each track and lend high confidence to the resulting positional accuracy of $\leq 0''.1$ in R.A. and 0″.1–0″.2 in decl. for GN 20.

The new astrometric coordinates allow us to compare the submillimeter source with high-resolution images in the publicly available deep *Spitzer* Infrared Array Camera (IRAC; Fazio et al. 2004) (Fig. 1*b*) and *Hubble Space Telescope* Advanced Camera for Surveys (*HST* ACS; Ford et al. 1998) (Fig. 1*c*) images of the GOODS-North field. The absolute astrometric accuracy of both of these images is ~0″.1, and they are both tied to the coordinate frame defined by the VLA positions in Richards (2000).[9] The IRAC 3.6 μm image reveals a source centered <0″.5 west of the submillimeter coordinates, while the higher resolution *HST V*-band image reveals a faint optical source 0″.8 to the west. From the analysis of available ACS images, it is found that this optical source is a *B*-dropout galaxy ($B = 27.2 \pm 0.4$, $V = 25.2 \pm 0.1$, $i = 24.4 \pm 0.1$), which gives constraints on the probable redshift to be $z \sim 3$–4. We believe that the 0″.8 offset between the SMA position and the *HST* position is significant, and there are several possible astrophysical explanations for this difference. The submillimeter emission may arise from part of a large galaxy where *V*-band emission is completely obscured. Alternatively, GN 20 might be an interacting system where the optical galaxy is a companion to the dusty, more actively star-forming galaxy. Although the observed FIR luminosities are significantly different, the apparent separation of these galaxies (~6 kpc at $z \sim 3$) suggests a close similarity to the Antennae system (NGC 4038/39), where the optical galaxies are separated by 7.5 kpc and where most of the starburst activity is occurring in the medium between the two galaxies (e.g., Wang et al. 2004).

GN 20 was suggested to be a two-component source, GN 20.1 (20.3 mJy) and GN 20.2 (11.7 mJy), separated by 18″ (140 kpc) in the low-resolution SCUBA image (Pope et al. 2005). The 890 μm flux agreement between our SMA observation and the SCUBA measurement of GN 20.1 implies that GN 20 may be a two-component source. However, the suggested position of GN 20.2 is beyond the half-power point of the SMA primary beam, where the sensitivity is reduced by more than a factor of 2. A detailed discussion in the context of multiwavelength observations of this source will be provided in a forthcoming paper (A. Pope et al. 2006, in preparation).

3.2. *MIPS J142824.0+352619 (MIPS-J1428)*

The SMA map of MIPS-J1428 is shown in Figure 1*d*. The derived total flux is 18.4 ± 2.5 mJy and shows excellent agreement with the 890 μm flux of 19.5 mJy extrapolated from the SCUBA 850 μm flux of 21.9 ± 1.3 mJy. MIPS-J1428 is not spatially resolved with the 2″.5 beam (see Fig. 2), and the derived coordinates from a point-source fit are $\alpha(2000) = 14^{h}28^{m}24^{s}.06$, $\delta(2000) = 35°26'19''.79$, with uncertainties in the fit of 0″.1 for both α and δ. The strong 890 μm detection allows us to make a higher resolution image using the visibilities of the longest baselines. The resulting 3 σ unresolved image provides us with a firm upper limit to the source size of $\leq 1''.2$ (10 kpc at $z = 1.325$), which is smaller than the size constraint given by the ~1″.5 VLA 1.4 GHz resolution.

The map of the test QSO 1419+543 after adding the two sidebands and two tracks is shown in the inset of Figure 1*d*. A point-source fit to the visibilities gave a positional offset from the phase center of $\Delta\alpha = 0''.11 \pm 0.05$ and $\Delta\delta = 0''.23 \pm 0.05$ for 1419+543. As with 1048+717 for GN 20, we fit a point-source model to the visibilities of 1419+543 in each sideband of each track separately. The results show that the offsets from the phase center had a wide range of values ($\Delta\alpha = 0''.04$–$0''.28$ and $\Delta\delta = 0''.13$–$0''.25$), with the overall average offset from the phase center of $\Delta\alpha = 0''.14 \pm 0.11$ and $\Delta\delta = 0''.21 \pm 0.05$. These uncertainties are larger than those found in 1048+717 for GN 20 and are slightly larger than the

[9] After applying the known positional offset in decl. of 0″.38 between the GOODS-N images and the VLA catalog positions (see http://data.spitzer.caltech.edu/popular/goods/Documents/ for details).

uncertainties expected from baseline errors. It is possible that other factors such as image smearing due to large phase noise may have introduced a small error in the source positions. Thus, we assess an uncertainty of ~0″.15 in R.A. and ~0″.2 in decl. for MIPS-J1428.

Figures 1*e* and 1*f* show the SMA 890 μm contours of MIPS-J1428 overlaid on the NDWFS *K*-band and *I*-band images. The astrometry of both of these images is tied to the reference frame defined by the USNO-A2.0 catalog, and the typical rms of the residuals is 0″.35 (B. T. Jannuzi et al. 2006, in preparation). The optical/NIR galaxy seen here is unambiguously the galaxy aligned with the strong submillimeter emission. The accurate astrometry of the submillimeter emission provided by the SMA allows tight constraints on the separation between the bright optical/NIR position and rules out fainter IRAC sources detected nearby (Borys et al. 2006). Hence, MIPS-J1428 could lie directly behind the foreground $z = 1.034$ galaxy, which would potentially result in a large amplification of the submillimeter source. Borys et al. (2006) use size/luminosity relationships to argue that despite the alignment, the amplification is likely modest since the Einstein ring is of comparable size to the known physical scales of local ultraluminous infrared galaxies (ULIRGs). Assuming that the lensing is modest, the size is comparable to that of other high-redshift submillimeter sources (Chapman et al. 2004). Using the star formation rate (SFR) estimated in Borys et al. (2006), our limit on the angular size, θ, of the object, we derive a lower limit on the SFR density of $>180(\theta/1.2)\mu^{-1}\ M_{\odot}\ \mathrm{yr}^{-1}\ \mathrm{kpc}^{-2}$, where μ is the lensing amplification. This is larger than local ULIRGs (Meurer et al. 1997) and comparable to other high-redshift submillimeter galaxies (Chapman et al. 2004).

4. SUMMARY

We present SMA observations of two 20 mJy submillimeter sources, GN 20 and MIPS-J1428. The positions of the submillimeter sources are determined with 0″.1–0″.2 accuracy with these data, allowing for precise identification of the correct optical galaxy counterpart to the bright submillimeter emission in GN 20 and providing evidence that the foreground lens is only weakly affecting the observed high FIR luminosity in MIPS-J1428. If many of the bright submillimeter galaxies are slightly lensed objects similar to MIPS-J1428, then the implied source counts of inherently bright submillimeter galaxies are overpredicted. Detailed studies, however, exist for only a few sources, and future surveys such as SHADES (Mortier et al. 2005) will provide important information about the star formation properties at high redshifts.

The Submillimeter Array is a joint project between the Smithsonian Astrophysical Observatory and the Academia Sinica Institute of Astronomy and Astrophysics, and is funded by the Smithsonian Institution and the Academia Sinica. This work made use of observations made with the *Spitzer Space Telescope*, which is operated by JPL, California Institute of Technology, under NASA contract 1407. This work made use of images provided by the NOAO Deep Wide-Field Survey (Jannuzi & Dey 1999), which is supported by the National Optical Astronomy Observatory (NOAO). NOAO is operated by AURA, Inc., under a cooperative agreement with the National Science Foundation.

REFERENCES

Barger, A. J., Cowie, L. L., & Richards, E. A. 2000, AJ, 119, 2092
Barger, A. J., Cowie, L. L., Sanders, D. B., Fulton, E., Taniguchi, Y., Sato, Y., Kawara, K., & Okuda, H. 1998, Nature, 394, 248
Borys, C., Chapman, S., Halpern, M., & Scott, D. 2003, MNRAS, 344, 385
Borys, C., et al. 2004, MNRAS, 352, 759
———. 2006, ApJ, 636, 134
Blain, A. W., Smail, I., Ivison, R. J., Kneib, J.-P., & Frayer, D. T. 2002, Phys. Rep., 369, 111
Chapman, S. C., Richards, E. A., Lewis, G. F., Wilson, G., & Barger, A. J. 2001, ApJ, 548, L147
Chapman, S. C., Smail, I., Windhorst, R., Muxlow, T., & Ivison, R. J. 2004, ApJ, 611, 732
Chapman, S. C., et al. 2003, ApJ, 585, 57
Cowie, L. L., Barger, A. J., & Kneib, J.-P. 2002, AJ, 123, 2197
Dowell, C. D., et al. 2003, Proc. SPIE, 4855, 73
Downes, D., et al. 1999, A&A, 347, 809
Dunlop, J. S., et al. 2004, MNRAS, 350, 769
Eales, S., Lilly, S., Webb, T., Dunne, L., Gear, W., Clements, D., & Yun, M. S. 2000, AJ, 120, 2244
Fazio, G. G., et al. 2004, ApJS, 154, 10
Ford, H. C., et al. 1998, Proc. SPIE, 3356, 234
Giavalisco, M., et al. 2004, ApJ, 600, L93
Greve, T. R., Ivison, R. J., Bertoldi, F., Stevens, J. A., Dunlop, J. S., Lutz, D., & Carilli, C. L. 2004, MNRAS, 354, 779
Ho, P. T. P., Moran, J. M., & Lo, K. Y. 2004, ApJ, 616, 1
Hughes, D. H., et al. 1998, Nature, 394, 241
Ivison, R. J., Smail, I., Le Borgne, J.-F., Blain, A. W., Kneib, J.-P., Bézecourt, J., Kerr, T. H., & Davies, J. K. 1998, MNRAS, 298, 583
Ivison, R. J., et al. 2002, MNRAS, 337, 1
Jannuzi, B. T., & Dey, A. 1999, in ASP Conf. Ser. 191, Photometric Redshifts and the Detection of High Redshift Galaxies, ed. R. J. Weymann et al. (San Francisco: ASP), 111
Johnston, K. J., et al. 1995, AJ, 110, 880
Meurer, G. R., Heckman, T. M., Lehnert, M. D., Leitherer, C., & Lowenthal, J. 1997, AJ, 114, 54
Mortier, A. M. J., et al. 2005, MNRAS, 363, 563
Pope, A., Borys, C., Scott, D., Conselice, C., Dickinson, M., & Mobasher, B. 2005, MNRAS, 358, 149
Richards, E. A. 2000, ApJ, 533, 611
Sault, R. J., Teuben, P. J., & Wright, M. C. H. 1995, in ASP Conf. Ser. 77, Astronomical Data Analysis Software and Systems IV, ed. R. A. Shaw, H. E. Payne, & J. J. E. Haynes (San Francisco: ASP), 433
Scott, S. E., et al. 2002, MNRAS, 331, 817
Smail, I., Ivison, R. J., & Blain, A. W. 1997, ApJ, 490, L5
Soifer, B. T., et al. 2004, BAAS, 204, 48.05
Wang, W.-H., Cowie, L. L., & Barger, A. J. 2004, ApJ, 613, 655
Wang, Z., et al. 2004, ApJS, 154, 193
Webb, T. M., et al. 2003, ApJ, 587, 41